

E. J. Padma Malar

Density functional theory analysis of some triple-decker sandwich complexes of iron containing *cyclo-P₅* and *cyclo-As₅* ligands

Received: 19 August 2004 / Accepted: 18 October 2004 / Published Online: 12 May 2005
© Springer-Verlag 2005

Abstract Structure and bonding in triple-decker cationic complexes $[(\eta^5\text{-Cp})\text{Fe}(\mu, \eta:\eta^5\text{-E}_5)\text{Fe}(\eta^5\text{-Cp})]^+$ (**1**: E = CH, **2**: E = P, **3**: E = As) and $[(\eta^5\text{-Cp})\text{Fe}(\mu, \eta:\eta^5\text{-Cp})\text{Fe}(\eta^5\text{-E}_5)]^+$ (E = P, As) are examined by density functional theory (DFT) calculations at the B3LYP/6-31+G* level. These species exhibit the lowest energy when all the three ligands are eclipsed. In the complexes with bifacially coordinated *cyclo-E₅*, the perfectly eclipsed *D_{5h}* sandwich structure **a** is found to be a potential minimum. The energy difference between the fully eclipsed and the staggered conformations **b** and **c** are within 1.0, 2.1, and 6.3 kcal/mol, respectively, for E = CH, P, and As. The isomeric species with monofacially coordinated *cyclo-E₅* (E = P, As), $[(\eta^5\text{-Cp})\text{Fe}(\mu, \eta:\eta^5\text{-Cp})\text{Fe}(\eta^5\text{-E}_5)]^+$ are predicted to be about 30 and 60 kcal/mol higher in energy, respectively, for E = P and As. The calculations predict that the bifacially coordinated *cyclo-E₅* (E = P, As) undergoes significant ring expansion leading to “loosening of bonds” as observed experimentally. The consequent loss of aromaticity in the central *cyclo-E₅* indicates that significant π -electron density from the ring can be directed towards bonding with the iron centers on both sides. The diffuse nature of the π -orbitals of *cyclo-P₅* and *cyclo-As₅* can lead to better overlap with the iron d-orbitals and result in stronger bonding. This is reflected in the bond order values of 0.377 and 0.372 for the Fe–P and Fe–As bonds in **2a** and **3a**, respectively. The natural population analysis reveals that the Fe atom that is coordinated to a *cyclo-E₅* (E = P, As) possesses a negative charge of –0.23 to –0.38 units due to transfer of electron density from the inorganic ring to the metal center.

Keywords Triple-decker · Sandwich complexes · *cyclo-P₅* · *cyclo-As₅* · electronic structure

E. J. Padma Malar
Department of Physical Chemistry, University of Madras,
Guindy Campus, Chennai-600025, India
E-mail: ejpmalar@yahoo.com

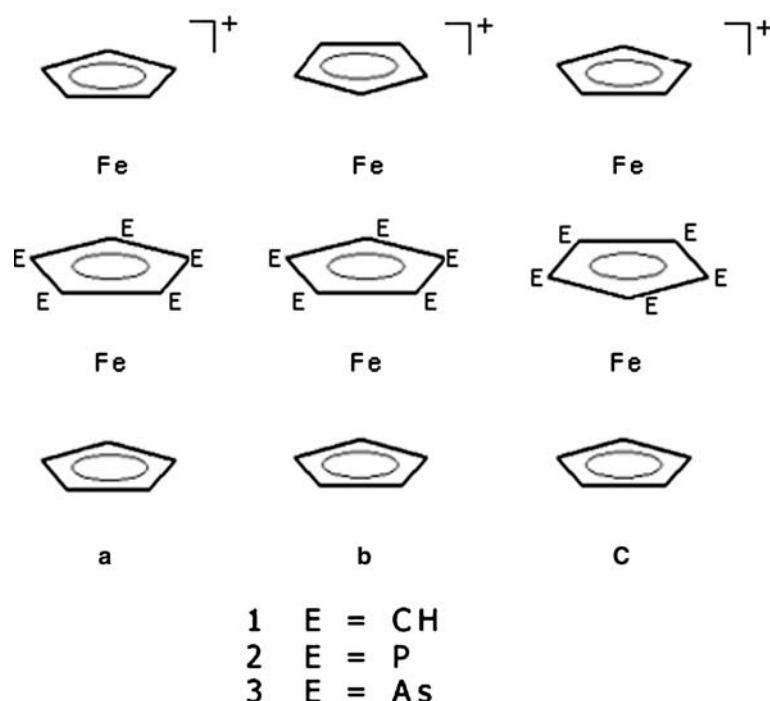
E. J. Padma Malar
University Grants Commission, New Delhi, India

1 Introduction

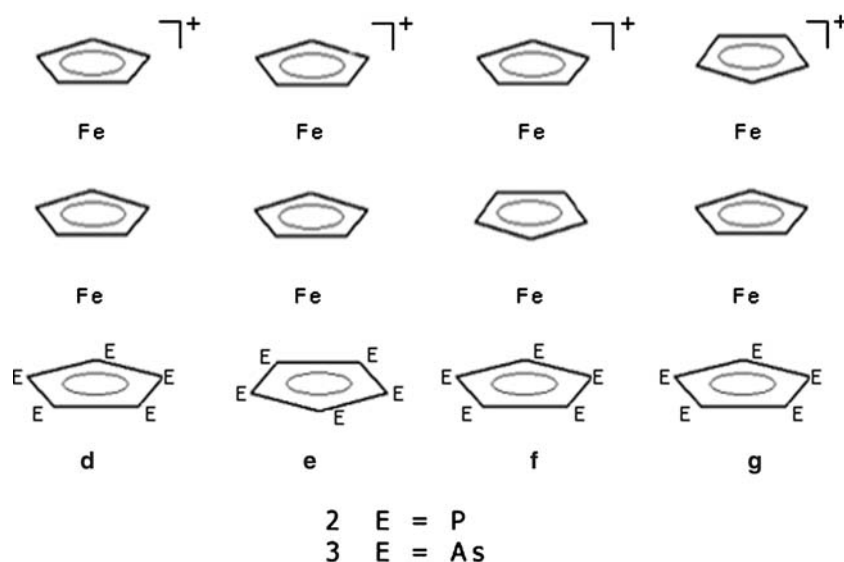
In the past two decades, a number of remarkable transition metal complexes containing homo-atomic rings E_n ($n = 3–6$) of Phosphorus and Arsenic were synthesized [1–6]. Ring systems such as P_4 , P_5 , P_6 , and As_5 are stabilized in the middle layer of triple-decker complexes $[(\eta^5\text{-L})\text{M}(\mu, \eta:\eta^n\text{-}E_n)\text{M}'(\eta^5\text{-L}')]^+$ (L, L' = C_5H_5 , C_5Me_5 , C_5Me_4Et ; M, M' = Ti, Fe, Co, Cr, Mo, W, V; E = P, As) [7–21]. In these triple-decker complexes, the terminal ligands L and L' are monofacially coordinated to one metal center by η^5 -coordination; the central *cyclo-E_n* ligand is bifacially coordinated to two metal centers by $\mu, \eta:\eta^n$ -coordination. Pentaphospholyl (*cyclo-P₅*) and its arsenic analogue are well studied [22–32] in mixed metallocenes $[(\eta^5\text{-L})\text{M}(\eta^5\text{-E}_5)]$. Carbon-free sandwich metallocenes $[\text{Ti}(\eta^5\text{-P}_5)_2]^{2-}$ and $[\text{Nb}(\eta^5\text{-As}_5)_2]^{3-}$ have been discovered very recently [33, 34]. These findings are of immense interest as they illustrate the potential of phosphorus and arsenic rings as ligands and can lead to a wealth of interesting transition metal complexes. Studies also show that these metallocenes and the triple-decker complexes form building blocks for multi-decker complexes [7, 10, 16, 35] and they have potential in the engineering of new materials.

Bonding in the triple-decker complexes containing E_n (E = P, As) in the middle deck is found to be different from the traditional triple-decker complexes $[\text{CpMCpMCp}]$ with central Cp ring. In some of these complexes, metal–metal bonding is present as evidenced by short M–M distances, which are in the bonding range [35]. The M–M distances in $[\text{LME}_n\text{ML}]$ are observed in the range 2.6–3.0 Å, which is much shorter than the value of about 3.4 Å in the complexes with central Cp rings [7, 10, 35]. Orbital interactions responsible for bonding in some triple-decker complexes with bridging E_n ligand were examined by Extended Hückel calculations [20, 35–38].

Although several triple-decker complexes with E_n rings in the middle layer have been investigated, so far there is no report on triple-decker complexes with *cyclo-E₅* in the terminal layer. A comparative study of the electronic structures



Scheme 1 Sandwich conformations of the triple-decker complexes with *cyclo-E*₅ in the middle deck



Scheme 2 Conformations of the triple-decker complex cations with *cyclo-E*₅ in the terminal deck

and bonding in triple-decker complexes having E_n ligand in the middle and in the terminal decks is expected to lead to an understanding of the origin of the preferential stability. In the present study, we have examined the molecular and electronic structures and nature of bonding in cationic triple-decker complexes of diiron $[(\eta^5\text{-Cp})\text{Fe}(\mu, \eta:\eta^5\text{-}E_5)\text{Fe}(\eta^5\text{-Cp})]^+$ and $[(\eta^5\text{-Cp})\text{Fe}(\mu, \eta:\eta^5\text{-Cp})\text{Fe}(\eta^5\text{-}E_5)]^+$, which contain a *cyclo-E*₅ ($E=\text{P}, \text{As}$) ligand in the middle and the terminal layer, respectively. The analogous carbocyclic complex species $[(\eta^5\text{-Cp})\text{Fe}(\mu, \eta:\eta^5\text{-Cp})\text{Fe}(\eta^5\text{-Cp})]^+$, **1**, is also investigated

for comparison. Schemes 1 and 2 show the systems under study. The parent triple-decker iron complex $[(\eta^5\text{-Cp})\text{Fe}(\mu, \eta:\eta^5\text{-Cp})\text{Fe}(\eta^5\text{-Cp})]\text{PF}_6$ was synthesized by Kudinov et al. [18] in 1999. Derivatives of **2**, $[(\eta^5\text{-Cp})\text{Fe}(\mu, \eta:\eta^5\text{-P}_5)\text{Fe}(\eta^5\text{-C}_5\text{Me}_4\text{R})]\text{PF}_6$ [$\text{R} = \text{CH}_3, \text{C}_2\text{H}_5$] were isolated and characterized by Scherer and coworkers [10]. Electrochemical properties and structures of Fe-Ru and diruthenium triple-decker salts, $[(\eta^5\text{-Cp})\text{Fe}(\mu, \eta:\eta^5\text{-P}_5)\text{Ru}(\eta^5\text{-Cp}^*)]\text{PF}_6$ and $[(\eta^5\text{-Cp}^*)\text{Ru}(\mu, \eta:\eta^5\text{-P}_5)\text{Ru}(\eta^5\text{-Cp}^*)]\text{PF}_6$ [$\text{Cp}^* = \text{C}_5\text{Me}_5$], were studied recently [16].

We have examined the electronic structures of the systems listed in Schemes 1 and 2 by the density functional theory (DFT) method [39,40], which is well known to yield results that are comparable with experimental findings in a variety of systems including organometallic compounds [41–46]. The recent DFT studies on metallocenes containing *cyclo*-P₅ ligand [33,47–51] have been successful in predicting their structural and bonding features. The dicationic triple-decker complex [CpCoAs₄CoCp]²⁺ has recently been characterized by DFT analysis by Von Hänisch et al. [21].

2 Computational Aspects

Hybrid Hartree–Fock–DFT calculations were performed with Becke’s three-parameter hybrid-exchange functional and the gradient-corrected nonlocal correlation functional of Lee, Yang, and Parr (B3LYP) [52,53], using the Gaussian 03 software [54]. We performed all electron calculations on the triple-decker complexes with the split valence basis set, which includes polarization and diffuse functions on the heavy atoms, at the B3LYP/6-31+G* level [55].

The triple-decker complexes with bifacially coordinated *cyclo*-E₅ were examined in three different sandwich conformations **a**, **b**, and **c** (Scheme 1). In the complexes with *cyclo*-E₅ in the periphery, four sandwich arrangements **d**, **e**, **f**, and **g** as, shown in Scheme 2, were studied. In all the structures, **a–g**, the centers of the middle ring and the two outer rings are collinear with the Fe–Fe centers.

The three ligands are eclipsed in the arrangement **a** with the D_{5h} point group while one pair of ligands is staggered in **b** which exhibits C_{5v} point group. In **c** all the three ligands are staggered with D_{5h} symmetry. The four conformations **d**, **e**, **f**, and **g** belong to the C_{5v} point group. Complete structural optimization was carried out for all the conformations **a–g**. At

the optimized geometries, vibrational frequencies were calculated and the total energies were corrected for zero-point vibrational energy (ZPE). The scaling factor of 0.98 for ZPE, which is reported to be suitable for B3LYP/6-31G* calculations [56], was used in the present work. The total energies of the cationic complexes and their ionic components $E(\text{Cp}^-)$, $E(E_5^-)$, and $E(\text{Fe}^{2+})$ are included in the supporting information (Table S1). The dication of iron was calculated at its ⁵D ground state. The quintuplet state is the lowest energy state of Fe²⁺ and the closed-shell singlet and the triplet states are higher in energy by 90.1 and 63.0 kcal/mol, respectively. Optimized Cartesian coordinates obtained by the B3LYP/6-31+G* method corresponding to potential minima of the triple-decker complexes are shown in supporting information.

3 Results and discussions

3.1 Energetics

The stabilization of the cationic triple-decker complex [(LFeL’FeL’’) ⁺] was calculated from the total energies of the ionic complex and the component species using the equation

$$\Delta E = E[(\text{LFeL}'\text{FeL}'')^+] - E(\text{L}^-) - E(\text{L}'^-) - E(\text{L}''^-) - 2E(\text{Fe}^{2+}).$$

Table 1 shows the binding energies, ΔE , of the different conformations of the triple-decker complexes examined in the present work at the B3LYP/6-31+G* level. The energy differences among the conformations **a**, **b**, and **c** in the carbocyclic complex **1** is predicted to be small (about 1 kcal/mol). However, the energy differences in the conformations **a**, **b**, and **c** for systems **2** and **3** are about 2.1 and 6.3 kcal/mol, respectively for E = P and As. The conformation **a**, in which the three ligands are eclipsed, exhibits the lowest energy in **1**, **2**, and **3** and is found to be the only potential minimum for the cationic complexes with *cyclo*-E₅ (E = CH, P, or As) in the middle layer. The conformation **c** in which the three ligands are staggered to each other has the highest energy among **a**, **b**, and **c** and it is a second-order saddle point. The conformation **b** with one pair of ligands staggered shows one imaginary vibrational frequency.

The finding that the eclipsed D_{5h} conformation **a** is the lowest energy potential minimum is in agreement with the observation of perfectly eclipsed sandwich geometry for the iron-ruthenium triple-decker complex cation [(η⁵-Cp)Fe(μ, η:η⁵-P₅)Ru(η⁵-Cp*)]⁺ by X-ray diffraction [16]. Even in the sandwich metallocenes M(Cp)₂ (M = V, Cr, Mn, Fe, Co, Ru, Os) [41–46,50] and the *cyclo*-P₅ analogues P₅MCp, M(P₅)₂ (M = Fe, Ru, Os) and [Ti(P₅)₂]²⁻ [33,47–50], the eclipsed sandwich structure is predicted to be the potential minimum and the staggered sandwich structure in most of the above systems is found to be a first-order saddle point by high-level DFT studies though the energy difference is about 1 kcal/mol. Indeed, the eclipsed structure was confirmed for ferrocene and ruthenocene by an electron diffraction study and a crystal structure analysis [57]. Since the small energy difference

Table 1 Binding energies in kcal/mol and the number of imaginary vibrational frequencies (hessian index) of the triple-decker sandwich complex cations at B3LYP/6-31+G* optimized geometries

System	Point group	Binding energy (Relative energy)	Hessian index
1a	D _{5h}	−1098.55 (0.0)	0
1b	C _{5v}	−1098.03 (0.52)	1
1c	D _{5h}	−1097.53 (1.02)	2
2a	D _{5h}	−1077.64 (0.0)	0
2b	C _{5v}	−1076.57 (1.07)	1
2c	D _{5h}	−1075.55 (2.09)	2
2d	C _{5v}	−1048.39 (29.25)	0
2e	C _{5v}	−1047.45 (30.19)	1
2f	C _{5v}	−1046.94 (30.70)	2
2g	C _{5v}	−1047.89 (29.75)	1
3a	D _{5h}	−1164.41 (0.0)	0
3b	C _{5v}	−1161.06 (3.35)	1
3c	D _{5h}	−1158.08 (6.33)	2
3d	C _{5v}	−1104.25 (60.16)	1
3e	C _{5v}	−1103.66 (60.75)	1
3f	C _{5v}	−1103.39 (61.02)	1
3g	C _{5v}	−1104.14 (60.27)	1

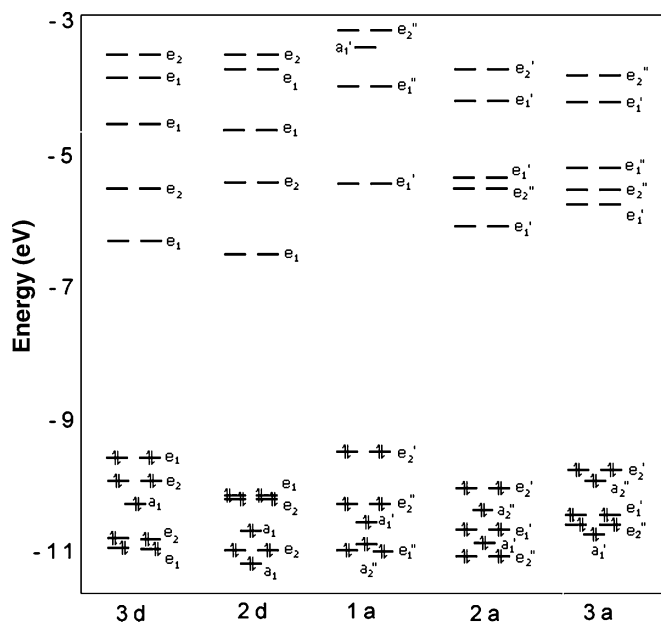


Fig. 1 B3LYP/6-31+G* energy level diagram showing the highest-occupied and lowest vacant molecular orbitals of the all-eclipsed triple-decker complex cations

of about 1 kcal/mol is within the numerical reliability of the computational method used, the relative energies of the conformers of **1** may not distinguish their stabilities. However, the calculated vibrational frequencies show that **1a** alone is a potential minimum. From this prediction and the observation of eclipsed sandwich structure in ferrocene [57], it may be inferred that the triple-decker complex cation $[\text{CpFeCpFeCp}]^+$ exists in the fully eclipsed conformer **1a**. Although the present analysis supports a perfectly eclipsed structure for the triple-decker complexes with bifacially coordinated *cyclo-E*₅, the crystal structure of related species $[(\eta^5\text{-Cp})\text{Fe}(\mu, \eta^5\text{-P}_5)\text{Fe}(\eta^5\text{-C}_5\text{Me}_4\text{Et})]^+$ has eclipsed Cp and *cyclo-P*₅ but the *cyclo-P*₅ and the *C*₅Me₄Et ligands are staggered [10]. The preference for the staggered arrangement between *cyclo-P*₅ and the *C*₅Me₄Et in the crystal structure may be due to the steric effect of ethyl substituent. Such staggered arrangements are also observed in the crystals of $[(\eta^5\text{-P}_5)\text{MFe}(\eta^5\text{-C}_5\text{Me}_4\text{Et})]$ (M = Fe, Ru) [22]

The four conformations **d**, **e**, **f**, and **g**, with *cyclo-E*₅ (*E* = P or As) as a terminal ligand, possess significantly higher energies than the lowest energy conformer **a** in which the *cyclo-E*₅ is bifacially coordinated. Thus, the conformations **2d**, **2e**, **2f**, and **2g** having $\eta^5\text{-P}_5$ are predicted to be about 30 kcal/mol higher in energy than **2a**. The conformations **3d**, **3e**, **3f**, and **3g** with a terminal $\eta^5\text{-As}_5$ are about 60 kcal/mol higher in energy than the conformation **3a**. Table 1 reveals that the conformation **d** in which all the three ligands are eclipsed possesses the lowest energy among the four conformations **d**, **e**, **f**, and **g**. The conformation **f** in which all the ligands are staggered has the highest energy. All the four conformations **d**, **e**, **f**, and **g** of the complex $[\text{As}_5\text{FeCpFeCp}]^+$ are predicted to be first-order saddle points. However, in the

analogous $[\text{P}_5\text{FeCpFeCp}]^+$, **2d** is a potential minimum, **2e** and **2g** are first-order saddle points and **2f** is a second-order saddle point.

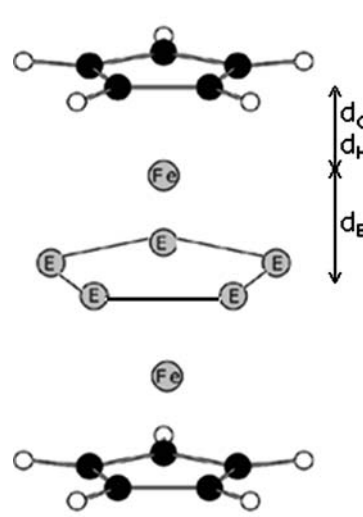
Figure 1 shows the energies of the highest occupied and lowest vacant MOs generated by the B3LYP/6-31+G* method in the all-eclipsed cationic species **1a**, **2a**, **3a**, **2d**, and **3d**. The origin of the preferential stability of the triple-decker complex with the *cyclo-E*₅ (*E* = P or As) middle deck over that in which it is the terminal deck can be understood in terms of orbital interactions. When the *cyclo-E*₅ (*E* = P or As) ligand is in the middle deck, the π -MOs can interact bifacially with the d-orbitals of the iron centers on either side. The diffuse nature of the *cyclo-E*₅ (*E* = P or As) orbitals results in better interactions with the metal orbitals and this is reflected by shorter Fe–*E*₅ separations than the Fe–Cp distance (Figs. 2 and 3). The stabilities of **2a** and **3a** are expected to be more than that of the corresponding species **2d** and **3d**, since the d-orbitals of two iron atoms interact with the orbitals of *cyclo-E*₅ in the former. The HOMO–LUMO energy gaps of **2a** and **3a** are 3.97 and 4.04 eV, respectively and are higher than the values of 3.53 and 3.22 eV in **2d** and **3d**. The larger HOMO–LUMO gaps in **2a** and **3a** reflect stronger metal ligand interactions than those in **2d** and **3d** and account for their preferential stability.

3.2 Structure and bonding

The present study shows only minor variations in the bond lengths and bond angles for the conformations **a**, **b**, and **c** of a given complex cation with bifacially coordinated *cyclo-E*₅ (*E* = CH, P or As). Similarly, the structural parameters of the conformations **d**, **e**, **f**, and **g** are predicted to be very similar. Selected structural parameters of the all-eclipsed conformations **a** and **d** are shown in Figs. 2 and 3, respectively.

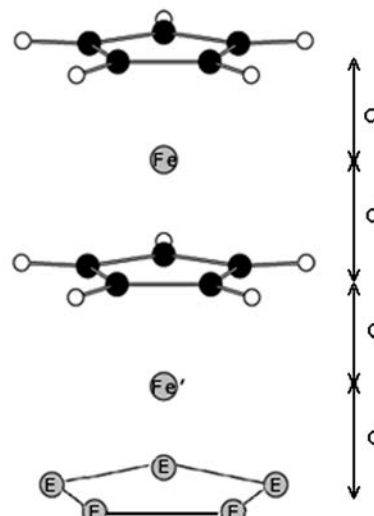
Figure 2 shows that the μ, η -coordinated Cp in the middle layer of **1a** undergoes ring expansion as compared to the terminal Cp. The C–C bond lengths in the terminal and the middle Cp rings in **1a** are 1.427 and 1.456 Å, respectively. The expansion of the central Cp in **1a** is accompanied by an increase in the corresponding Fe–C and the Fe–Cp (*d*_c) distances. The covalent bond orders [58,59], calculated in terms of natural atomic orbitals [60,61], show that the C–C bonds in the central Cp have lower bond orders of 1.191 than the value of 1.272 in the terminal Cp. This indicates that the bonding in the bifacially coordinated Cp is weaker than that in the monofacially coordinated Cp.

Structural features around the terminal and central Cp rings in the species **2d** and **3d** (Fig. 3) are predicted to be very similar to that of **1a** as the electronic environments are similar. The P–P bond lengths of the monofacially coordinated P₅ ligand and the distance from its center to Fe' (*d*_p) are 2.140 and 1.596 Å, respectively in **2d**. The above P–P and *d*_p lengths are very close to the corresponding values of 2.142 and 1.592 Å predicted by B3LYP/6-311+G* for CpFeP₅ [50], as expected from their similar electronic environments. The P–P and the *d*_p lengths in **2d**, predicted by



	1a	2a	3a
E	CH	P	As
C—C	1.427 (1.272)	1.426 (1.275)	1.427 (1.274)
E—E	1.456 (1.191)	2.170 (1.003)	2.341 (0.979)
Fe—C	2.068 (0.348)	2.095 (0.307)	2.083 (0.304)
Fe—E	2.090 (0.234)	2.428 (0.377)	2.536 (0.372)
d_C	1.674	1.708	1.693
d_E	1.684	1.578	1.570
d_H	1.649	1.695	1.702
θ	1.6	0.8	-0.6

Fig. 2 Selected structural parameters in the triple-decker cationic species **1a**, **2a**, and **3a**. Distances are in Å and bent angle θ is in degrees



	2d	3d
E	P	As
C—C	1.426 (1.271)	1.427 (1.271)
(C—C) _m	1.454 (1.196)	1.454 (1.190)
E—E	2.140 (1.185)	2.333 (1.158)
Fe—C	2.070 (0.350)	2.068 (0.350)
Fe—C _m	2.087 (0.231)	2.088 (0.228)
Fe'—C _m	2.128 (0.217)	2.095 (0.225)
Fe'—E	2.421 (0.451)	2.516 (0.442)
d_C	1.677	1.674
d_{Cm}	1.682	1.683
$d_{Cm'}$	1.732	1.687
$d_{E'}$	1.596	1.547
θ	1.7	1.2
θ'	1.5	-0.3

Fig. 3 Selected structural parameters in the triple-decker cationic species **2d** and **3d**. Distances are in Å and bent angle θ is in degrees

the present B3LYP/6-31+G* calculations, are about 0.04 and 0.06 Å longer than those in the crystal structure of $[(\eta^5\text{-C}_5\text{Me}_4\text{Et})\text{Fe}(\eta^5\text{-P}_5)]$ [22]. In **3d**, the As—As and the d'_{As} distances are 2.333 and 1.547 Å respectively. The bond orders of the P—P and Fe'—P bonds in **2d** are 1.185 and 0.451 while those of the As—As and Fe'—As bonds in **3d** are 1.158 and 0.442.

Comparison of the structures of **2a** and **2d** shows that the bifacially coordinated *cyclo*-P₅ in **2a** is expanded significantly with an increase of about 0.03 Å in the P—P lengths. The predicted P—P bond lengths of 2.170 Å in the central *cyclo*-P₅ ligand is in good agreement with the observed values of 2.157 and 2.156 Å in the related systems $[(\eta^5\text{-Cp})\text{Fe}(\mu, \eta:\eta^5\text{-P}_5)\text{Ru}(\eta^5\text{-Cp}^*)]\text{PF}_6$ and $[(\eta^5\text{-Cp}^*)\text{Ru}(\mu, \eta:\eta^5\text{-P}_5)\text{Ru}(\eta^5\text{-$

Table 2 Relative % aromaticity of Cp and E_5 ligands in the triple-decker complex species^[a]

System	Cp ligand		E_5 ligand Terminal
	Terminal	Middle	
1a	63.4	41.0	
2a	64.2		
3a	63.9		
2d	63.1	42.4	39.1
3d	63.1	40.8	32.8

[a] B3LYP/6-31+G* bond orders: C–C in Cp[−] = 1.405; C–C in ethane = 1.042;

P–P in *cyclo*-P₅ anion = 1.408; As–As in *cyclo*-As₅ anion = 1.396

Cp*)PF₆ by single-crystal X-ray diffraction [16]. The experimental observation of elongated P–P lengths for the central *cyclo*-P₅ in [(η^5 -Cp)Fe(μ , η : η^5 -P₅) Ru(η^5 -Cp*)]⁺ and [(η^5 -Cp*)Ru(μ , η : η^5 -P₅) Ru(η^5 -Cp*)]⁺ as compared to the P–P lengths of about 2.10 Å in [(η^5 -C₅Me₄Et)M(η^5 -P₅)] (M = Fe, Ru) [22] is attributed to apparent “loosening of bonds” upon bifacial coordination [16]. The covalent bond orders for the P–P bonds in **2a** are 1.003. These bond order values reveal that the ring bonds of the central *cyclo*-P₅ are characteristic of single bonds and the π -bonding may be cutoff. According to the ring current definition of Jug [62, 63], it may be inferred that aromaticity is lost in the P₅ ring when it is bifacially coordinated. The As–As bond lengths in **3a** are elongated by 0.008 Å as compared to the bonds in the terminal *cyclo*-As₅ of **3d**. However, the bond orders show that the central As₅ ring is non-aromatic like the *cyclo*-P₅ in **2a**.

Even though the *cyclo*-P₅ anion is predicted to be as aromatic as cyclopentadienyl anion [64–67], our recent B3LYP/6-311+G* study [50] showed that the P₅ ring retains about 45% aromaticity as compared to the free anionic ring in CpFeP₅ and (P₅)₂Fe. The aromaticity of the Cp ring is about 66% in ferrocene and pentaphospha ferrocene [50]. As a consequence, considerable π -electron densities from the Cp and *cyclo*-P₅ rings are directed towards bonding with the metal center. Although the bond orders of the central *cyclo*-E₅ (E = P, As) show that these rings are nonaromatic, the ring bonds are delocalized in the remaining ligands. The relative aromaticity RI_x of these ligands in the triple-decker complexes is estimated with reference to the free anionic ligand, using the relationship [50]

$$RI_x = \frac{I_x(\text{complex}) - I_{\text{ethane}}}{I_x(\text{anion}) - I_{\text{ethane}}},$$

where x denotes the ligand moiety and I_x denotes its aromaticity index [68]. I_{ethane} is the C–C bond order in the nonaromatic compound ethane. Table 2 lists the relative aromaticities of the ligand moieties in the fully eclipsed complexes studied. It is seen that the terminal Cp ligands of the triple-decker complex cations retain 63–64% aromaticity while the middle layer of Cp rings exhibit only 41–42% aromaticity. Though aromaticity is lost in the *cyclo*-P₅ and *cyclo*-As₅ ligands when bifacially coordinated, they possess 39 and 33% relative aromaticity in the complexes **2d** and **3d**, respectively.

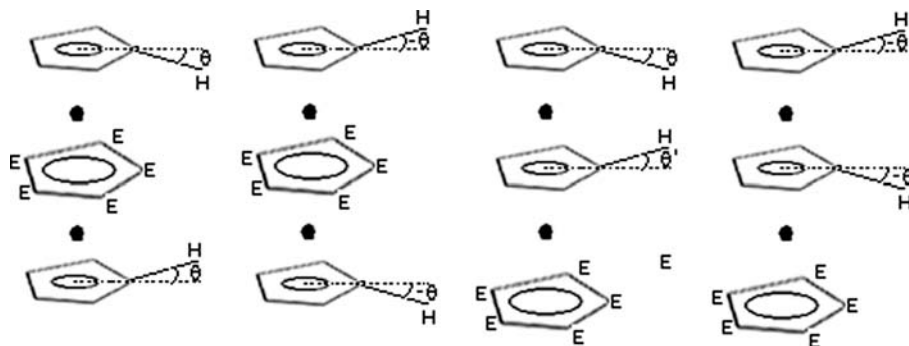
One of the unique features of the triple-decker complexes with central *cyclo*-E_n (E = P, As) ligand is the observation of short metal – metal distances [7, 10, 16, 35]. The observation of “loosening of bonds” and the consequent loss of aromaticity in the central P₅ and As₅ rings implies that significant π -electron densities from these rings can be directed towards bonding with the metal center. Further, the diffuse nature of the π -orbitals of *cyclo*-P₅ and *cyclo*-As₅ can lead to better overlap with the iron d-orbitals and result in stronger bonding. This is reflected in the larger bond order values of 0.377 and 0.372 for the Fe–P and Fe–As bonds in **2a** and **3a**, respectively, than the value of 0.234 for the corresponding Fe–C bonds in **1a**. The stronger bonding between the metal center and the *cyclo*-E₅ (E = P, As) brings the ligand closer to the metal. The distances between the central *cyclo*-E₅ and the iron are $d_P = 1.578$ and $d_{As} = 1.570$ Å in **2a** and **3a**, respectively, and are considerably shorter than the corresponding distance of 1.684 Å between central Cp and Fe in **1a**. The d_P value of 1.578 Å in **2a** is comparable with the experimental value of about 1.54 Å observed in the related triple-decker systems [10, 16]. The predicted d_C distance of 1.708 Å in **2a** also agrees with the experimental values of 1.679 Å [10] and 1.687 Å [16]. The distance between the two iron centers in **1a**, **2a**, and **3a** are 3.368, 3.156, and 3.140 Å, respectively. Although the Fe–Fe distances in **2a** and **3a** are about 0.2 Å shorter than in **1a**, they are about 0.47 Å longer than the sum of covalent radii (2.68 Å) and the possibility of metal – metal bonding is ruled out in these systems.

3.2.1 Bending of Hydrogens in the Triple-decker Complexes

In sandwich metallocenes, both experiments and calculations provide evidences that the hydrogen atoms of the Cp ring are bent from the plane of the carbon atoms, either towards the metal or away from the metal center by 3.0–6.5 degrees [69–76]. So far, there is no report regarding the bending of hydrogens in the Cp ring of triple-decker complexes. The present B3LYP/6-31+G* calculations show that the hydrogens of the terminal and central Cp rings of the different conformers of **2** and **3** under study are bent. Scheme 3 defines the bend angles θ and θ' . The present study shows that θ and θ' vary between -2 and 2° for the different conformations examined.

Figure 2 reveals that the hydrogens of the η^5 -coordinated Cp rings are bent towards Fe atom (θ positive) in **1a** and **2a** by 1.6 and 0.8°. Consequently, the d_H distances are shortened by 0.025 and 0.013 Å in **1a** and **2a** as compared to the corresponding d_C distances (Fig. 2). The bend angle of 1.6° in **1a** is very close to the theoretically predicted value of 1.5° [50] and the value of 1.6(4)° reported by neutron diffraction study in ferrocene [76]. Our study shows that in the complex with μ , η -As₅, **3a**, the hydrogens are bent away from the metal center by 0.6°.

In the carbocyclic complex cation, **1**, the hydrogens of the bifacially coordinated central Cp do not bent at all (θ' is zero) in the perfectly eclipsed conformation **1a** and in the



Scheme 3 Definition of bend angles θ and θ'

all-staggered arrangement **1c**. In **1b**, the bending of the hydrogens in the μ, η -Cp is negligibly small (bend angle = 0.1°). The hydrogens of the terminal and the central Cp ligands of **2d** bend like in ferrocene ($\theta = 1.7^\circ$; $\theta' = 1.5^\circ$). In **3d**, the hydrogens of the terminal Cp bend towards iron by 1.2° but the bend angle θ' is -0.3° .

4 Natural population analysis

The electronic population of the valence orbitals of the metal centers and the ligand atoms of the triple-decker complexes are examined by natural population analysis (NPA) using the natural atomic orbital (NAO) basis [60, 61]. Table 3 presents the valence orbital populations and the net NPA charges on the atomic centers. The calculations show that the 3d- and 4s-populations of the iron atom are about 7.4 and 0.2 electrons when it is sandwiched between two Cp ligands. The total valence population of these iron centers is about 7.65 electrons, which is less than the free-atom population of eight electrons and the iron possesses NPA charge of about +0.35 units. On the other hand, the 3d- and 4s-populations of the iron that is sandwiched between a Cp ligand and an E_5 ($E = \text{P, As}$) ring is about 7.8–7.9 and 0.4 electrons, respectively. Thus, the total valence population at the Fe center that is coordinated to a *cyclo- E_5* ($E = \text{P, As}$) ligand exceeds eight electrons, resulting in a net charge of -0.23 to -0.38 units at Fe. The total valence population of each E atom of *cyclo- E_5* ($E = \text{P, As}$) is less than five electrons and is positively charged (+0.11 – 0.26). Even though the triple-decker complexes under investigation are mono-cationic species, the B3LYP/6-31+G* calculations predict that the iron center is negatively charged when it is coordinated to a *cyclo- E_5* ($E = \text{P, As}$) ligand. In our earlier study [50], the electronic population analysis in bis(*cyclo- P_5*) M ($M = \text{Fe, Ru, Os}$) led to an uncommon observation that the metal center attains a negative charge of almost one unit due to a transfer of about 0.1 electron from each phosphorus in the ligand to the metal. The present NPA analysis corroborates the above finding. A comparative analysis using the *cyclo- P_5* and the *cyclo- As_5* ligands reveals that their electronic properties are similar and both these ligands transfer electron density to the metal center in the complexes.

Table 3 Natural population of valence orbitals of the ligand and metal atoms and their natural charges

System	Element ^a	Natural Population			Net NPA charge
		4s	4p	3d	
1a	C _m	0.98	3.30		-0.30
	Fe	0.20	0.01	7.43	0.35
2a	P	1.64	3.15		0.22
	Fe	0.36	0.04	7.90	-0.30
3a	As	1.70	3.05		0.26
	Fe	0.38	0.03	7.96	-0.38
2d	P	1.67	3.22		0.11
	Fe	0.19	0.02	7.44	0.35
	Fe'	0.36	0.06	7.80	-0.23
3d	As	1.74	3.12		0.14
	Fe	0.19	0.02	7.43	0.35
	Fe'	0.40	0.04	7.91	-0.35

^a C_m denotes the carbon in the middle Cp layer

5 Conclusions

The B3LYP/6-31+G* calculations predict that the cationic complex, $[(\eta^5\text{-Cp})\text{Fe}(\mu, \eta:\eta^5\text{-}E_5)\text{Fe}(\eta^5\text{-Cp})]^+$ (**1**: $E = \text{CH}$, **2**: $E = \text{P}$, **3**: $E = \text{As}$), exhibits the lowest energy in the perfectly eclipsed D_{5h} sandwich structure **a**, which is found to be a potential minimum. The energy difference between the fully eclipsed and the staggered conformations **b** and **c** are within 1.0, 2.1, and 6.3 kcal/mol, respectively, for $E = \text{CH, P, and As}$. The isomeric species with monofacially coordinated *cyclo- E_5* ($E = \text{P, As}$), $[(\eta^5\text{-Cp})\text{Fe}(\mu, \eta:\eta^5\text{-Cp})\text{Fe}(\eta^5\text{-}E_5)]^+$, also possess lowest energies when all the three ligands are eclipsed (conformation **d**). Conformation **d** is a potential minimum for $E = \text{P}$ but 30 kcal/mol higher in energy than **2a**. When $E = \text{As}$, the conformation **3d** is found to be a first-order saddle point and it is about 60 kcal/mol higher in energy than **3a**.

The present calculations predict that the bifacially coordinated *cyclo- P_5* in **2a** undergoes significant ring expansion leading to “loosening of bonds” as observed experimentally. The situation is similar in the complex **3a** having a central *cyclo- As_5* ligand. The consequent loss of aromaticity in the central *cyclo- E_5* indicates that a significant π -electron density from the ring can be directed towards bonding with the iron centers on both sides. Further, the diffuse nature of the π -orbitals of *cyclo- P_5* and *cyclo- As_5* can lead to better overlap

with the iron d-orbitals and result in stronger bonding. This is reflected in the larger bond order values of 0.377 and 0.372 for the Fe–P and Fe–As bonds in **2a** and **3a**, respectively, than the value of 0.234 for the corresponding Fe–C bonds in **1a**. The larger HOMO–LUMO energy gaps in **2a** and **3a** as compared to the values in **2d** and **3d** reflect that stronger metal–ligand interactions are present in the former complexes.

It is seen that the terminal Cp ligands of the triple-decker complex cations retain 63–64% aromaticity while the middle layer of Cp rings exhibit only 41–42% aromaticity. Though aromaticity is lost in the cyclo-P₅ and cyclo-As₅ ligands when bifacially coordinated, they possess 39 and 33% relative aromaticity in the complexes **2d** and **3d**, respectively.

Hydrogens of the η^5 -coordinated terminal Cp rings are bent towards Fe atom in **1a** and **2a** but they are bent away from Fe in **3a** when cyclo-As₅ is the central ligand. The natural population analysis reveals that the Fe center that is coordinated to a cyclo-E₅ (E = P, As) possesses a net charge of -0.23 to -0.38 units due to transfer of electron density from cyclo-E₅ ligand to the metal center.

References

- Scherer OJ (1987) Comments Inorg Chem 6:1
- Scherer OJ (1990) Angew Chem Int Ed Engl 29:1104–1122
- Baudler M, Glinka K (1993) Chem Rev 93:1623
- Scherer OJ (1999) Acc Chem Res 32:751
- Whitemire KH (1998) Adv Organomet Chem 42:1
- Dillon KB, Mathey F, Nixon JF (1998) Phosphorus: the carbon copy, Wiley, Chichester
- Scherer OJ, Schwab J, Wolmershäuser G, Kaim W, Gross R (1986) Angew Chem Int Ed Engl 25:363
- Scherer OJ, Schwab J, Swarowsky H, Wolmershäuser G, Kaim W, Gross R (1988) Chem Ber 121:443–449
- Scherer OJ, Sitzmann H, Wolmershäuser G (1985) Ang Chem Int Ed Engl 24:351
- Scherer OJ, Brück T, Wolmershäuser G (1989) Chem Ber 122:2049–2054
- Scherer OJ, Wiedemann W, Wolmershäuser G (1989) J Organomet Chem 361: C 11
- Scherer OJ, Rink B, Heckmann G, Wolmershäuser G (1992) Chem Ber 125:1011
- Scherer OJ, Pfeiffer K, Wolmershäuser G (1992) Chem Ber 125:2367
- Scherer OJ, Schwarz G, Wolmershäuser G (1996) Z Anorg Allg Chem 622:951–957
- Herberhold M, Frohmader G, Milius W (1996) J Organomet Chem 522:185–196
- Kudinov AR, Loginov DA, Starikova ZA, Petrovskii PV, Corsini M, Zanella P (2002) Eur J Inorg Chem 2002:3018
- Hughes AK, Murphy VJ, O'Hare D (1994) J Chem Soc Chem Comm 1994:163
- Kudinov AR, Petrovskii PV, Rybinskaya MI (1999) Russ Chem Bull 48:1352,1362
- Scherer OJ, Pfeiffer K, Wolmershäuser G (1992) Chem Ber 125:2367
- Reddy AC, Jemmis ED, Scherer OJ, Winter R, Heckmann G, Wolmershäuser G (1992) Organomet 11:3894
- Von Hänisch C, Fenske D, Weigend F, Ahlrichs R (1997) Chem Eur J 3:1494
- Scherer OJ, Brück T, Wolmershäuser G (1988) Chem Ber 121:935–938
- Scherer OJ, Blath C, Wolmershäuser G (1990) J Organomet Chem 387: C 21
- Baudler M, Etbach (1991) Angew Chem Int Ed Engl 30:580
- Avent AG, Geoffrey F, Cloke N, Flower KR, Hitchcock PB, Nixon JF (1994) Angew Chem Int Ed Engl 33:2330
- Hitchcock PB, Jones C, Nixon JF (1994) Angew Chem Int Ed Engl 33:463
- Detzel M, Mohr T, Scherer OJ, Wolmershäuser G (1994) Ang Chem Int Ed Engl 33:1110–1112
- Scherer OJ, Hilt T, Wolmershäuser G (1998) Organomet 17:4110
- Scherer OJ, Wiegel S, Wolmershäuser G (1998) Chem Eur J 4:1910–1916
- Rink B, Scherer OJ, Wolmershäuser G (1995) Chem Ber 128:71–84
- Herber RH, Scherer OJ (2000) Inorg Chim Acta 308:116–120
- Herber RH, Scherer OJ (2000) Eur J Inorg Chem 2000:2451–2453
- Urnezis E, Brennessel WW, Cramer CJ, Ellis JE, Schleyer PvR (2002) Science 295:832
- Kesanli B, Fettingner J, Scott B, Eichhorn B (2004) Inorg Chem 43:3840–3846
- Jemmis ED, Reddy AC (1990) Proc Indian Acad Sci (Chem Sci) 102:379–393 and the references cited therein
- Di Vaira M, Sacconi L (1982) Angew Chem Int Ed Engl 21:330
- Tremel W, Hoffmann R, Kertesz M (1989) J Am Chem Soc 111:2030
- Jemmis ED, Reddy AC (1988) Organometallics 7:1561
- Hohenberg P, Kohn W (1964) Phys Rev B 136:864
- Parr RG, Yang W (1989) Density functional theory of atoms and molecules. Oxford University, New York
- Orendt AM, Facelli JC, Jiang YJ, Grant DM (1998) J Phys Chem A 102:7692
- Matsuzawa N, Seto J, Dixon DA (1997) J Phys Chem A 101:9391
- Mayor-López MJ, Weber J (1997) Chem Phys Lett 281:226
- Maron L, Eisenstein O (2000) J Phys Chem A 104:7140
- Kaupp M, Schleyer PvR, Dolg M, Stoll H (1992) J Am Chem Soc 114:8202
- Xu Z-F, Xie Y, Feng W-L, Schaefer III HF (2003) J Phys Chem A 107:2716
- Frison G, Mathey F, Sevin A (2002) J Phys Chem A 106:5653
- Frunzke J, Lein M, Frenking G (2002) Organometallics 21:3351
- Lein M, Frunzke J, Frenking G (2003) Inorg Chem 42:2504
- Malar EJP (2004) Eur J Inorg Chem 2004:2723–2732
- Malar EJP (2003) Inorg Chem 42:3873
- Becke AD (1993) J Chem Phys 98:5648
- Lee C, Yang W, Parr RG (1988) Phys Rev B 37:785
- Frisch MJ, Trucks GW, Schlegel HB, Scuseria GE, Robb MA, Cheeseman JR, Montgomery JA Jr, Vreven T, Kudin KN, Burant JC, Millam JM, Iyengar SS, Tomasi J, Barone V, Mennucci B, Cosi M, Scalmani G, Rega N, Petersson GA, Nakatsuji H, Hada M, Ehara M, Toyota K, Fukuda R, Hasegawa J, Ishida M, Nakajima T, Honda Y, Kitao O, Nakai H, Klene M, Li X, Knox JE, Hratchian HP, Cross JB, Adamo C, Jaramillo J, Gomperts R, Stratmann RE, Yazyev O, Austin AJ, Cammi R, Pomelli C, Ochterski JW, Ayala PY, Morokuma K, Voth GA, Salvador P, Dannenberg JJ, Zakrzewski VG, Dapprich S, Daniels AD, Strain MC, Farkas O, Malick DK, Rabuck AD, Raghavachari K, Foresman JB, Ortiz JV, Cui Q, Baboul AG, Clifford S, Cioslowski J, Stefanov BB, Liu G, Liashenko A, Piskorz P, Komaromi I, Martin RL, Fox DJ, Keith T, Al-Laham MA, Peng CY, Nanayakkara A, Challacombe M, Gill PMW, Johnson B, Chen W, Wong MW, Gonzalez C, Pople JA (2003) Gaussian 03 Revision B04, Gaussian Inc, Pittsburgh
- Foresman JB, Frisch A (1996) Exploring chemistry with electronic structure methods; Gaussian, Inc: Pittsburgh
- Bauschlicher CW, Patridge H (1995) J Chem Phys 103:1788
- a) Haaland A, Nilsson JE (1968) Acta Chem Scand 22:2653; b) Haaland A (1979) Acc Chem Res 12:415
- Wiberg KB (1968) Tetrahedron 24:1083
- Gopinathan MS, Jug K (1983) Theor Chim Acta 63:511
- Reed AE, Weinstock RB, Weinhold F (1985) J Chem Phys 83:735
- Reed AE, Curtiss LA, Weinhold F (1988) Chem Rev 88:899
- Jug K (1983) J Org Chem 48:1344
- Jug K, Köster A (1991) J Phys Org Chem 4:163
- Baudler M, Akpapoglou S, Ouzounis D, Wasgestian F, Meinigke B, Budzikiewicz H, Munster H (1988) Angew Chem Int Ed Engl 27:280

-
65. Malar EJP(1992) *J Org Chem* 57:3694
 66. Hamilton TP, Schaefer HF (1989) *Ang Chem Int Ed Engl* 28:485
 67. Dransfeld A, Nyulaszi L, Schleyer PvR (1998) *Inorg Chem* 37:4413
 68. In the present analysis, the aromaticity index is taken as the lowest ring bond-order, in accordance with the ring-current definition of Jug [62,63]
 69. Waterman KC, Streitwieser A, Blom R, Faegri K Jr, Midtgaard T (1991) *J Am Chem Soc* 113:3230
 70. Bohn RK, Haaland A (1966) *J Organomet Chem* 5:470
 71. Drouin BJ, Cassak PA, Kukolich SG (1997) *Inorg Chem* 36:2868
 72. Jutzi P, Khol F, Hofmann P, Kruger C, Tsay YH (1980) *Chem Ber* 113:757
 73. Alexandratos S, Streitwieser A Jr, Schaefer HF III (1976) *J Am Chem Soc* 98:7959
 74. Jespersen KK, Chandrashekar J, Schleyer PvR (1980) *J Org Chem* 45:1608
 75. Waterman KC, Streitwieser A Jr (1984) *J Am Chem Soc* 106:3138
 76. Takusagawa F, Koetzle TF (1979) *Acta Crystallogr B* 35:1074